4-23-2013

Laser flash synthesis of graphene and its inorganic analogues: An innovative breakthrough with immense promise

Prashant Kumar
Birck Nanotechnology Center, Purdue University, kumar131@purdue.edu

Kumar, Prashant, "Laser flash synthesis of graphene and its inorganic analogues: An innovative breakthrough with immense promise" (2013). *Birck and NCN Publications.* Paper 1327.
http://dx.doi.org/10.1039/c3ra41149d

RSC Advances

RSC Publishing

REVIEW

View Article Online
View Journal | View Issue

Cite this: *RSC Advances*, 2013, **3**, 11987

Laser flash synthesis of graphene and its inorganic analogues: An innovative breakthrough with immense promise

Prashant Kumar*

Laser-based green synthetic approaches for 2D atomic sheets of graphene, graphene nanoribbons and inorganic analogues of graphene are relatively new techniques. There are several significant laser-based approaches for graphene synthesis such as (a) laser exfoliation, (b) intercalation and exfoliation in liquid nitrogen, (c) pulsed laser deposition, (d) laser induced ultrafast chemical vapour deposition, (e) laser induced catalyst-free growth of graphene from solid carbon sources, (f) epitaxial graphene growth on a Si rich surface of SiC by laser sublimation of surface silicon atoms, (g) reduction of graphene oxide and (h) unzipping of carbon nanotubes. Apart from the deoxygenation of graphene, lasers have also been employed for the dehydrogenation and dehalogenation of graphene surfaces. Such laser induced bond dissociation paves the way for achieving the desired band gap in graphene by adequately controlling the extent of such surface bonds. Such photochemical transformations can be exploited for patterning and nanolithography of graphene and related materials. Laser exfoliation has successfully been extended to synthesize inorganic analogues of graphene such as 2D atomic sheets of hexagonal BN and metal dichalcogenides such as MoS_2, $MoSe_2$, WS_2, WSe_2 *etc*. It is noteworthy that the emerging novel laser-based approaches have tremendously simplified the synthesis of 2D atomic sheets and are capable of yielding impurity-free device quality 2D materials in a scalable manner and consequently inspiring various commercial applications of such materials. An overview of the progress made into laser based approaches is presented.

Received 10th March 2013,
Accepted 23rd April 2013

DOI: 10.1039/c3ra41149d

www.rsc.org/advances

1. Introduction

Graphene, a 2D flatland, has come a long way from being a dream material to the realization of its many advanced technological applications. After its discovery,[1] the world has not looked back and graphene has now been established as a unique nanomaterial.[2–5] Within a short space of time, it has been proven to be one of the ''wonder materials'' of the 21st century and as a material it is expected to be developed even further in future.[6–8] Properties including atomically thin layers with high mobility,[9] mechanical strength,[10] optical transparency,[11] tunability of the band-gap by doping[12] and by external fields[13] make graphene unique in many ways. Therefore, it is not surprising that graphene has been used in a broad spectrum of applications such as in general electronics[14,15] and flexible electronics in particular,[16] spintronics,[17–19] data storage,[20] NEMS,[21,22] as a thermally conducting material,[23] as a thermoelectric material,[24] as a corrosion resistant material,[25] in photonics,[26] in optoelectronics,[27–30] as a laser material,[31] in OLEDs,[32] in chemical sensors,[33] bio-sensors,[34] supercapacitors,[35,36] batteries[37] and in general as an energy material,[38] in

Birck Nanotechnology Centre, Purdue University, West Lafayette, Indiana, USA-47906. E-mail: kumar131@purdue.edu; magmemory@gmail.com

Prashant Kumar

Dr Prashant Kumar, broadly a nanotechnology practitioner, is currently working at Birck Nanotechnology Centre of Purdue University in the USA. He has primary research interests in understanding and exploiting laser–matter interactions spanning photo-physics and photo-chemistry. He has employed lasers for various pursuits including synthesis of 2D materials as well as metallic nanoparticles, nanopatterning, defect engineering, crystallization of amorphous thin films and for lasing action in semiconductor nanocrystals. Presently he is involved in laser-based nanomanufacturing of nanowires and 2D materials and their multilayers. He is a member of the Royal Society of Chemistry and life member of the American Physical Society and American Nano Society.

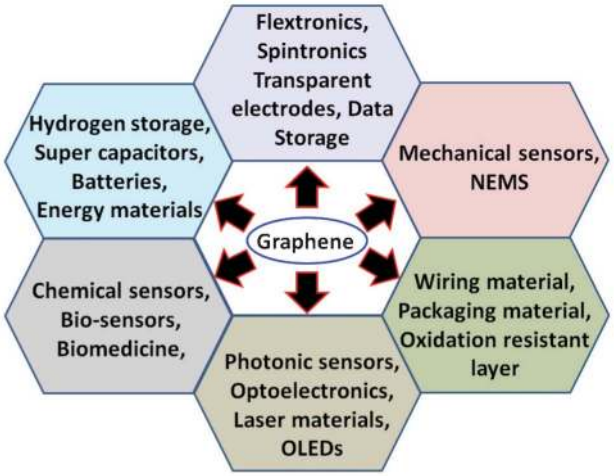

Fig. 1 Applications of graphene.

hydrogen storage[39,40] and in biomedicine.[41] Fig. 1 showcases some significant applications of the "wonder material" graphene.

Graphene was first obtained *via* a micromechanical cleavage technique using scotch tape.[1] However, with its overwhelming application potential, the need for a large scale production method was felt and therefore various chemical routes for the synthesis of graphene were developed over time. Among the many approaches for graphene synthesis, a few significant ones are the exfoliation of graphite,[42–46] intercalation and exfoliation of graphite,[47,48] arc discharge of graphite in the presence of helium and hydrogen gases,[49] chemical vapour deposition,[11,50–52] epitaxial graphene growth *via* sublimation of silicon from SiC,[53–55] from solid carbon sources[56–58] and graphene oxide reduction.[59–61] Graphene nanoribbons are long sheets of graphene with limited widths, due to which they exhibit fascinating behaviour, even better than graphene in some cases. Oxidative unzipping of CNTs yields graphene nanoribbons.[62,63] Reaction with molecular hydrogen can also convert CNTs into graphene nanoribbons.[64] Defects have a huge role to play in the process of unzipping CNTs.[65,66] Fig. 2 summarizes some of the significant synthetic approaches for graphene. The success of graphene has prompted the development of some inorganic analogues, a class of materials which are inspired by graphene, yet are different from graphene as far as the materials properties are concerned. These inorganic analogues do not suffer from the zero band gap problem in their intrinsic forms, which has been a roadblock for the application of graphene for semiconductors. Graphene-like 2D sheets of insulating boron nitride (BN), and semiconducting materials such as metal dichalcogenides *e.g.* MoS_2, $MoSe_2$, WS_2, WSe_2 *etc.* have already been synthesized[67–69] by exfoliation and it is expected that many more 2D materials will soon follow suit.

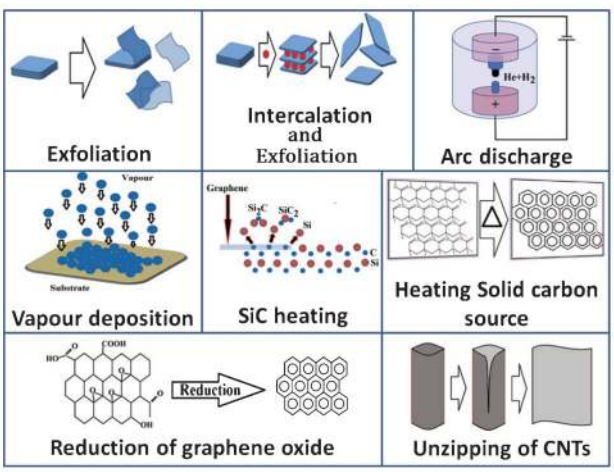

Fig. 2 Synthetic approaches for graphene.

Due to the ever-broadening scope of graphene, graphene nanoribbons and their inorganic analogues for real life applications, there is an urgent need for technological advances to simplify the synthetic strategies. Lasers, as optical energy sources, are available in a wide range of wavelengths (IR to deep UV), a broad variation in pulse widths (down to femtoseconds) and laser beam fluences varying from μJ cm^{-2} to several J cm^{-2} without the use of an external converging lens which can, as a matter of fact, be used to further tune the laser fluence. Also, lasers are available in continuous wave form as well as in the form of pulsed laser beams (repetition rate from 1 Hz to several kHz). Increasing the energy per photon would enable the breakage of stronger chemical bonds and higher beam fluence would give rise to higher local temperature. Higher repetition rate is another parameter which provides heating and cooling cycles. Thus, due to the great deal of freedom in the selection of laser parameters provided by a laser as an energy source, one can conveniently create a unique set of exotic physical and chemical conditions exactly suitable for a particular photophysical or photochemical transformation to occur. To drive photophysical transformations, such as exfoliation of 2D atomic sheets from its bulk counterpart, or photochemical transformations, such as breaking chemical bonds (*e.g.* deoxygenation or dehydrogenation), a particular set of conditions for laser fluence, pulse width, total energy delivered to the sample and repetition rate would be needed. Also, there will be a defined window for a particular laser parameter, for example laser fluence, which would provide suitable conditions. Laser processing is emerging as a powerful technique for material manipulation in general[70–75] and for carbon materials[76] in particular. Laser-based clean optical techniques therefore seem to have huge application potential for quick and scalable synthesis of impurity free 2D atomic sheets of graphene and its inorganic analogues. In this article, we review laser-based synthetic approaches for graphene, graphene nanoribbons and inorganic analogues of graphene.

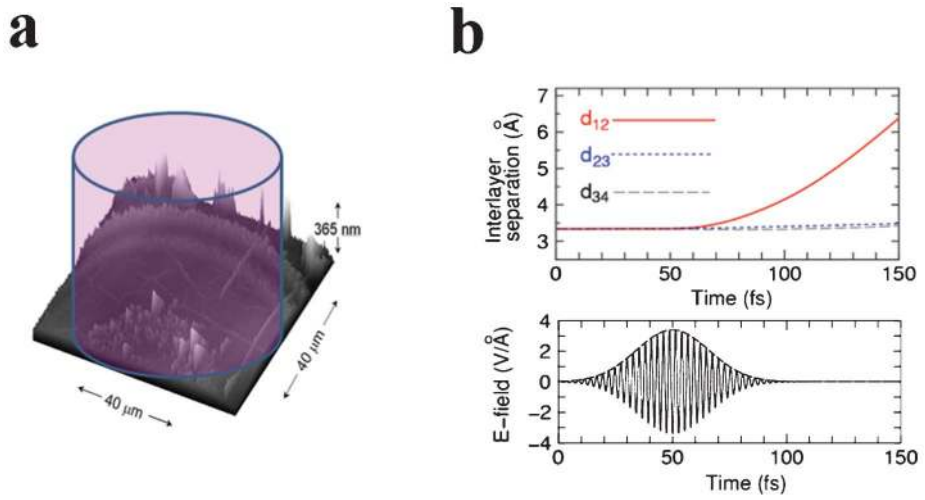

Fig. 3 (a) Spatial features formed on a graphite surface using a fs laser. Reprinted with permission from ref. 77. Copyright 2009, American Physical Society. (b) Interlayer separation increase (exfoliation) as a function of time due to fs laser irradiation on graphite studied by an *ab initio* method. Reprinted with permission from ref. 78. Copyright 2010, American Physical Society.

2. Exfoliation of graphite

Ultrafast single-shot femtosecond laser ablation of graphite was reported in 2009 to result in the detachment of charged graphene nanoflakes.[77] Fig. 3(a) depicts the kind of spatial surface features formed due to laser shock. The decay of the transient surface charge suggested that detachment of graphene was possible *via* non-thermal pathways. The lattice dynamics of the surface was successfully tracked *in situ via* time-resolved Coulomb explosion efficiency measurements. Laser induced repulsive forces and intrinsic attractive forces thus compete with each other. Hence, the critical point where the laser would be successful in exfoliating the topmost graphene layer would occur when both these forces are equal. Thus, to be precise, the phenomenon of exfoliation is athermal and laser shock is required to give rise to suitable conditions for exfoliation. Later on, an *ab initio* study was carried out to better understand the athermal exfoliation of graphite by ultrashort femtosecond laser ablation to achieve 2D atomic sheets of graphene.[78] An external electric field with polarization normal to the graphite surface was considered to interact with solid graphite. To simulate the process, an ultrashort field pulse was used for the calculation and it was shown that such an electric field pulse would kick start the process of exfoliation of the outermost layer from the adjacent layer just beneath it, as shown in Fig. 3(b). Since most of the femtosecond lasers are micron diameter beams, the process would occur on a pretty small scale. However, such preliminary studies laid the foundations of photo exfoliation.

Etching of the topmost graphene layer in already synthesized graphene by CVD was achieved *via* laser-induced oxidative burning[79] in a confocal Raman instrument. The exfoliation conditions were attained when the topmost graphene layer had high laser absorption and the bottom layer of graphene worked as a heat sink. The phenomenon of oxidative etching was closely monitored *in situ* by G-band mapping using confocal Raman spectroscopy, which uses a 532 nm laser with power $>$ 60 mW and a scanning speed in the range of a few micrometers per second. The G-band shift is indicative of heat accumulation. Also, as can be observed in Fig. 4, the thinned region (image b) exhibits a down shift in the G′-band, compared to that for pristine graphene (image a) grown by CVD. Laser exfoliation of a highly ordered pyrolytic graphite (HOPG) target in a PLD chamber using a Nd–YAG laser (532 nm, 7 ns) has been reported to yield few layer graphene (close to 10 layers) films.[80] The 2D-band shift was monitored in the process, which was triggered at a laser fluence of 5 J cm^{-2}. Fig. 5 shows the TEM image and Raman spectra of few layer graphene films obtained by this approach. The effects of laser fluence and the substrate–target distance on the end product were studied. Products so formed were collected on a silicon substrate. It was observed that the product consists of few layer graphene, amorphous carbon and graphite films. Further, laser exfoliation of a HOPG target fixed at the bottom of a vessel filled with deionized water has recently been reported to yield graphene oxide.[81] Fig. 6(a)–(c) show the process of graphene layer formation at an air/water interface. The obtained product is confirmed to be graphene oxide as it exhibits absorption at $\sim$260 nm (see Fig. 6(d)) and shows photoluminescence in the visible region with a peak around 420 nm.

We have recently carried out detailed experiments on the laser exfoliation of graphite in various media. Among the various solvents tested, the use of DMF, being a polar solvent which heavily interacts with graphitic systems, for laser exfoliation of graphite has been observed to yield single- and few-layer graphene.[4] Typically, 4 mg of graphite powder dispersed in 4 ml of DMF taken in a quartz vessel is irradiated by a Lambda Physik KrF excimer laser (λ = 248 nm, τ = 30 ns) with a laser fluence of 1.5 J cm^{-2} and at a repetition rate of 5

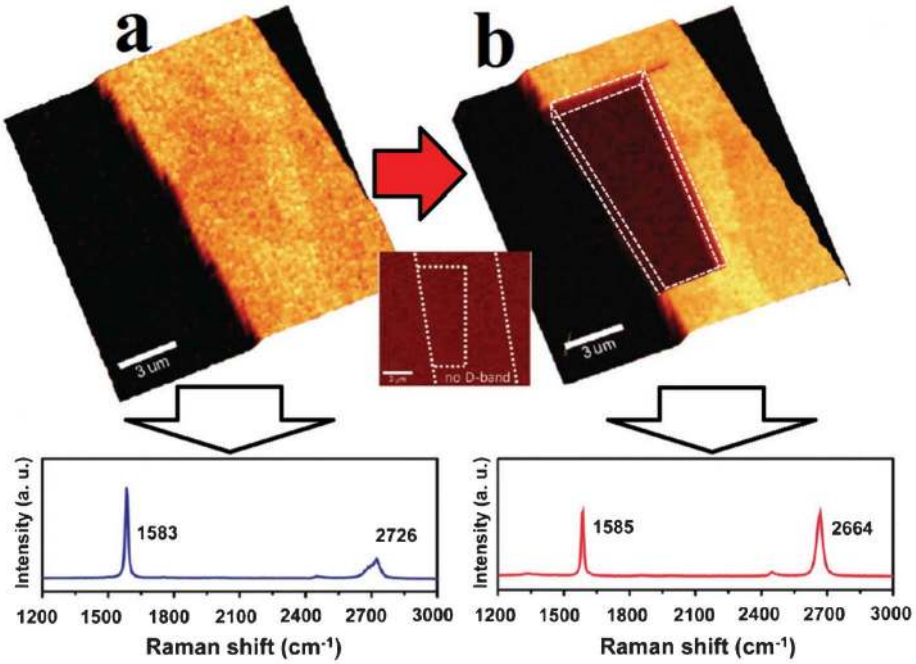

Fig. 4 Laser thinning of graphene obtained by a CVD technique. Confocal Raman mapping (a) before and (b) after the laser thinning experiment. Reprinted with permission from ref. 79. Copyright 2011, American Chemical Society.

Hz for 1 h. The dispersion was magnetically stirred during the irradiation. The irradiated dispersion was centrifuged at 3000 rpm for 5 min and the top one-third was transferred to a separate container. It was found that this supernatant liquid was stable for a prolonged duration. When the supernatant liquid was subsequently characterized, it was observed to be mostly 1–3 layers of graphene sheets. Suitable centrifugation can be employed to filter out the single layered graphene sheets. The dispersion of graphite powder in DMF before laser irradiation was black and the supernatant fluid obtained after the laser irradiation and centrifugation was transparent (See Fig. 7(a)). Fig. 7(b), (c) and (e) are typical FESEM, TEM and AFM images of the obtained graphene sheets. The TEM images reveal that laser exfoliated graphene is quite transparent and is therefore only a few layers thick. The AFM image reveals the presence of two-dimensional flakes up to a few hundred nm in lateral dimensions. The AFM height profile of the largest circular sheet, shown in Fig. 7(f), corresponds to single layer graphene. The typical Raman spectrum of the obtained graphene is shown in Fig. 7(g). Thus, laser exfoliation has been proven to be a novel, quick, single-step exfoliation technique to yield impurity free graphene. The lateral dimensions of the obtained graphene depend on the laser parameters used for the purpose. Extreme laser fluence tends to break graphene sheets into pieces and thus nanosheets can be obtained. The average lateral dimension of graphene decreases with increasing laser fluence as shown in Fig. 7(d). The lateral dimension would also depend on the laser pulse rate and the duration of exfoliation.

3. Intercalation and exfoliation

Laser-induced intercalation and exfoliation of graphite, employing a Q-switched pulsed Nd–YAG nanosecond laser in a liquid nitrogen medium, has recently been reported.[82] When solid graphite is immersed in liquid nitrogen, liquid nitrogen seeps through the atomic carbon layers and at such a cryogenic temperature, the lattice vibrations are reduced. As shown in the schematic in Fig. 8(a), as soon as the laser is exposed to graphite immersed in liquid nitrogen, the liquid nitrogen converts to gas and expands, creating a spontaneous explosive outward force which is greater than the intrinsic attractive forces between the layers of atomic sheets of carbon. Fig. 8(b) and (c) show the SEM image and Raman spectra, respectively, for few layer graphene. This experiment demonstrates a controlled cryogenic laser-induced intercalation and exfoliation method to synthesize graphene.

4. Epitaxial growth of graphene on silicon carbide

Growth of epitaxial graphene (EG) on the Si rich face of SiC has been known for a while *via* thermal treatment methods. Laser exposure would make surface conversion to graphene from SiC rather convenient as controlled laser exposure would not harm the layer underneath or other device components. Thus laser induced epitaxial graphene synthesis is a desirable technique. Recently, excimer laser irradiation of n-type 4H–SiC (0001) has been employed to achieve graphene.[83] Laser fluence was observed to determine the thickness of the graphene film

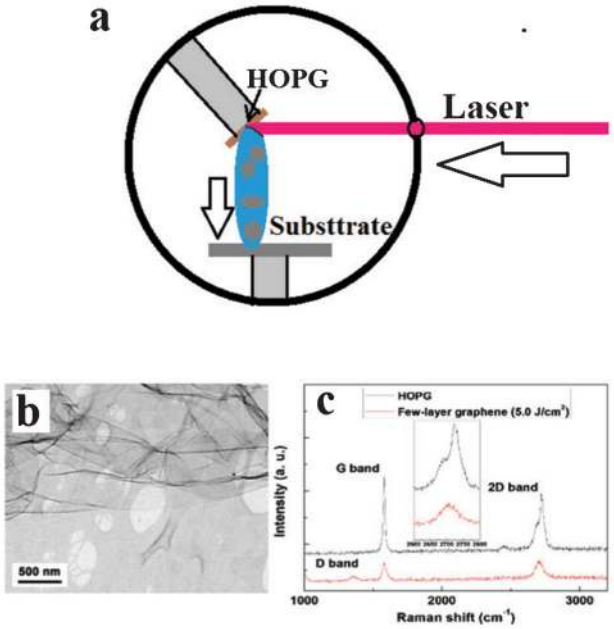

Fig. 5 Laser exfoliation of a HOPG target in a PLD chamber. (a) Schematic of the experiment, (b) the TEM image and (c) the Raman spectra of graphene deposited on the substrate due to the exfoliation process. Reprinted with permission from ref. 80. Copyright 2011, American Institute of Physics.

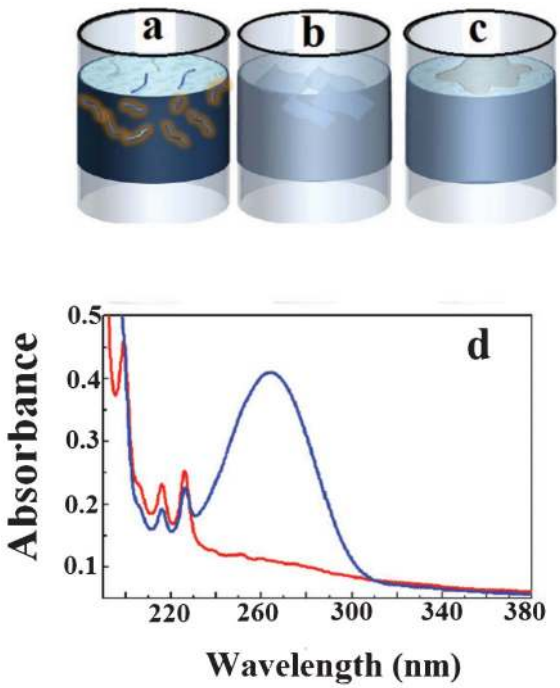

Fig. 6 Graphene oxide obtained by laser exfoliation of HOPG in deionized water. (a)–(c) Schematic of the process of graphene oxide layer formation at a liquid/air interface, and (d) the absorption spectra for the as-formed graphene oxide. Reprinted with permission from ref. 81. Copyright 2012, Institute of Physics, London.

down to a single monolayer. Laser-synthesized graphene does not exhibit Bernal stacking and surface reconstruction of the SiC surface underneath, which are otherwise reported in the case of thermally treated SiC. Fig. 9(a) and (b) shows the FESEM image and Auger mapping of patterned graphene achieved by masked laser irradiation. The red and yellow colours in Fig. 9(b) correspond to single- and bi-layer graphene. Fig. 9(c) shows the STM image with feature heights of 0.3–0.4 nm and Fig. 9(d) shows the atomic resolution STM image of the as-formed graphene. Laser synthesized epitaxial graphene is observed to have a greater surface area covered by single layer graphene compared with the thermally grown epitaxial graphene. This technique does not need ultra high vacuum (UHV), which otherwise is essential. Moreover, the laser based technique is quite fast.

5. Pulsed laser deposition (PLD)

In line with chemical vapour deposition of graphene, physical vapour deposition of graphene has already been reported.[84–86] Graphite is usually used as a target in UHV pulsed laser deposition chambers, and the substrate used is a transition metal surface (as shown in Fig. 10(a)). A considerably higher substrate temperature (1300 °C) was reported to yield high quality 1–2 layer graphene (see Fig. 10(b)).[84] Higher substrate temperatures yield graphene growth directly on the transition metal catalyst without any carbide formation at the interface between graphene and the transition metal, which otherwise is the case.[84] The choice of catalyst layer is still under discussion. Various transition metals are currently being employed as catalysts for this purpose, but nickel metal appears to be the best for yielding graphene at low temperatures. Laser parameters like the cooling rate and laser fluence also affect the quality of the graphene films.[86]

6. Laser induced chemical vapour deposition (LCVD)

A continuous wave (CW) laser (λ = 532 nm) has been used for laser-induced chemical vapour deposition in an environmental chamber.[87,88] The laser power used for this purpose was 5 W and Ni foil was used as the substrate. Methane and H_2 were used as the precursor gases in a volume ratio 5 : 2. Higher laser scan speed yielded a lower number of graphene layers. The LCVD process follows a vapor–liquid–solid (VLS) mechanism and the process takes only nanoseconds or picoseconds to complete, which thus leads to ultrafast growth of graphene. Fig. 11(a) shows a schematic diagram of direct writing of graphene using the LCVD technique. Fig. 11(b) shows the Raman spectra of different numbers of graphene layers achieved *via* LCVD. The excellent 2D Raman peak intensity for single layer graphene in Fig. 11(b) shows that graphene synthesized *via* this technique has excellent 2D crystallinity. One of the advantages of this technique is that a laser with a

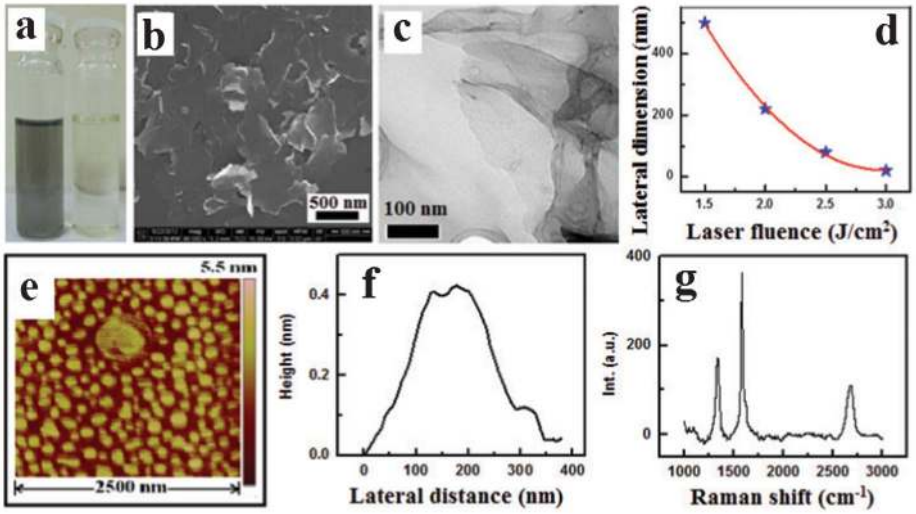

Fig. 7 Laser exfoliation of graphene; (a) a photograph of a graphite dispersion in DMF solvent (left) and the supernatant achieved after centrifugation of the laser irradiated dispersion (right), (b) FESEM, (c) TEM, and (e) AFM images, (f) the height profile of the largest graphene sheet in the AFM image and (g) the Raman spectrum of graphene obtained by laser exfoliation. The lateral dimension of graphene *vs.* laser fluence used for exfoliation is shown in (d). (Author's original research).

desired beam area can be scanned on a metal catalyst surface and thus direct graphene lithography can be realized. The beam area can be reduced by focusing it, which would yield higher power, or by the convenient use of a pin-hole mask. The absence of a D peak in the Raman spectra of LCVD graphene in contrast to the usual CVD technique showcases the superior quality (the defect free nature) of the obtained graphene.

7. From solid carbon sources

Lasers can, in principle, transform solid carbon sources to graphene. Apart from conventional transition metal templates, silicon[89] and quartz[90] have recently been used as substrates for coating solid carbon sources, and laser irradiation capable of dissociating solid carbon sources and also melting silicon or quartz gives rise to a new mechanism of graphene growth, which has not been explored so far by any other techniques. Fig. 12 and Fig. 13 show laser spots on solid carbon sources

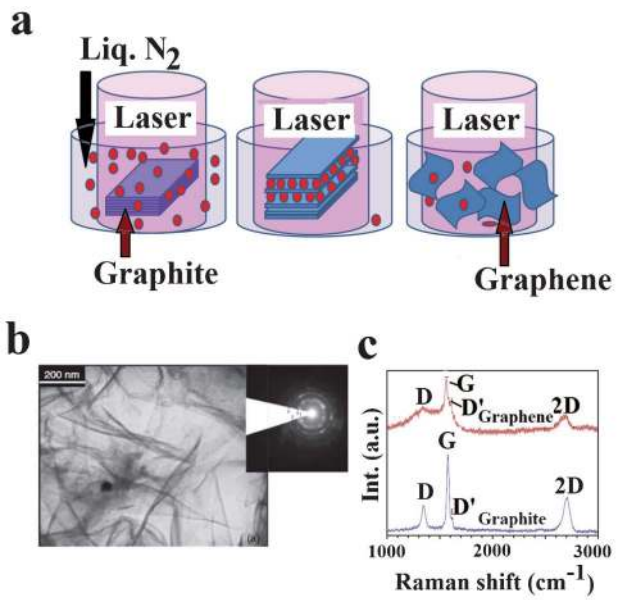

Fig. 8 Intercalation and exfoliation of graphite in a liquid nitrogen medium. (a) Schematic of the experiment, (b) the TEM image and electron diffraction pattern, (c) the Raman spectra for graphene and the parent graphite. Reprinted with permission from ref. 82. Copyright 2012, Astro Ltd.

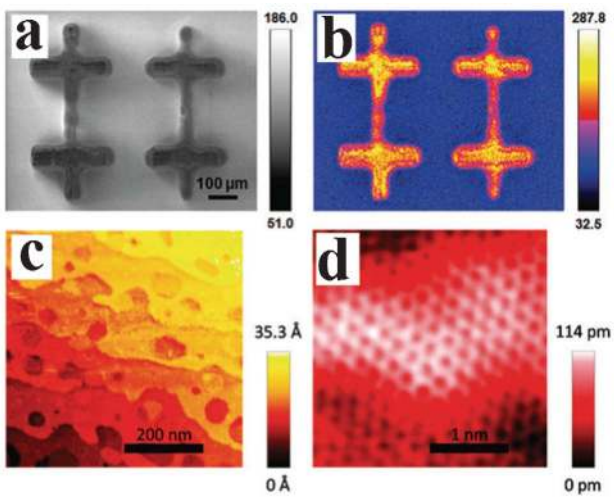

Fig. 9 Laser irradiation induced epitaxial growth of graphene on SiC. (a) FESEM image and (b) Auger mapping of patterned graphene achieved by masked laser irradiation. The red and yellow colours in (b) correspond to single- and bi-layer graphene. STM images of the as-formed graphene at (c) lower resolution and (d) atomic resolution. Reprinted with permission from ref. 83. Copyright 2010, American Chemical Society.

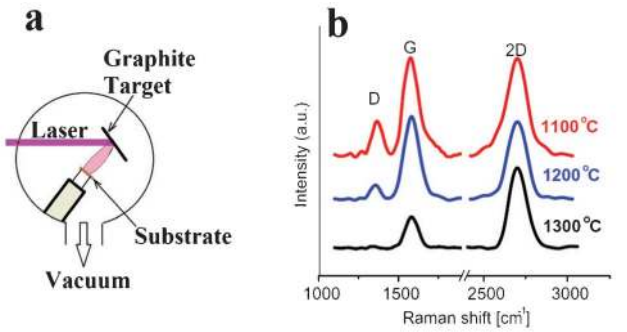

Fig. 10 Pulsed laser deposition of graphene. (a) Schematic of the PLD technique and (b) the dependence of the Raman spectra on substrate temperature. Reprinted with permission from ref. 84. Copyright 2010, Elsevier.

and the corresponding Raman spectra for silicon and quartz substrates, respectively. It was observed that laser fluence is of the utmost importance as a parameter. At fluence below the melting points of the silicon or quartz substrates, no graphene growth is observed. Also, there is an upper limit for power and time of exposure, above which graphene layers are not obtained. The graphene growth mechanism is: (a) dissociation of the solid carbon source into carbon atoms, (b) dissolution of the carbon atoms into a molten pool of silicon or quartz, and (c) diffusion of the carbon atoms back to the top surface to construct a graphene lattice while cooling takes place. This emerging laser-based technique demonstrates the metal catalyst-free growth of graphene. The electrical conductivity

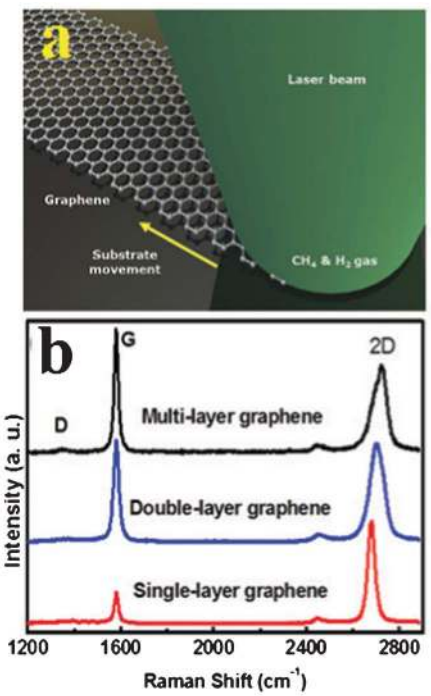

Fig. 11 (a) Schematic diagram of the LCVD technique and (b) the Raman spectra for different numbers of graphene layers. Reprinted with permission from ref. 87. Copyright 2011, American Institute of Physics.

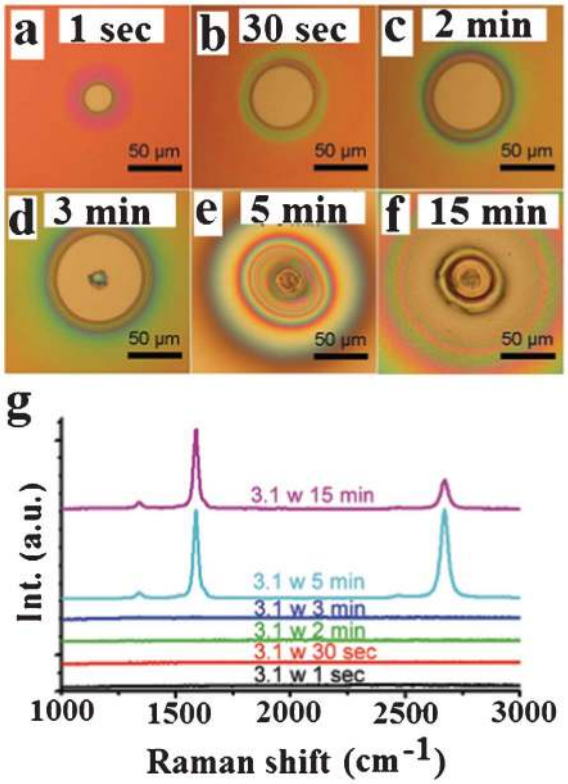

Fig. 12 Laser induced growth of graphene from PMMA on a silicon substrate; (a)–(f) laser spots with varying laser irradiation times and (g) Raman spectra for different laser irradiation times at a fixed laser power of 3.1 W. Reprinted with permission from ref. 89. Copyright 2012, American Institute of Physics.

of this catalyst-free graphene is comparable to those obtained *via* chemical techniques.[90] One of the advantages with this technique is that graphene transfer from the metal catalyst layer to the random substrate for a particular application

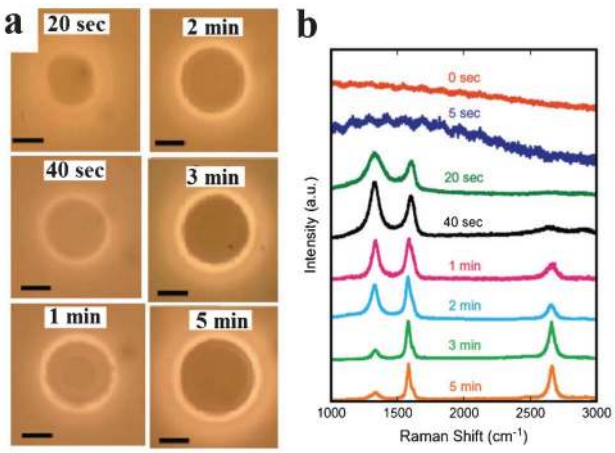

Fig. 13 Laser induced growth of graphene from PMMA on a quartz substrate; (a) laser spots with varying laser irradiation times and (b) Raman spectra for different laser irradiation times. Reprinted with permission from ref. 90. Copyright 2013, Elsevier.

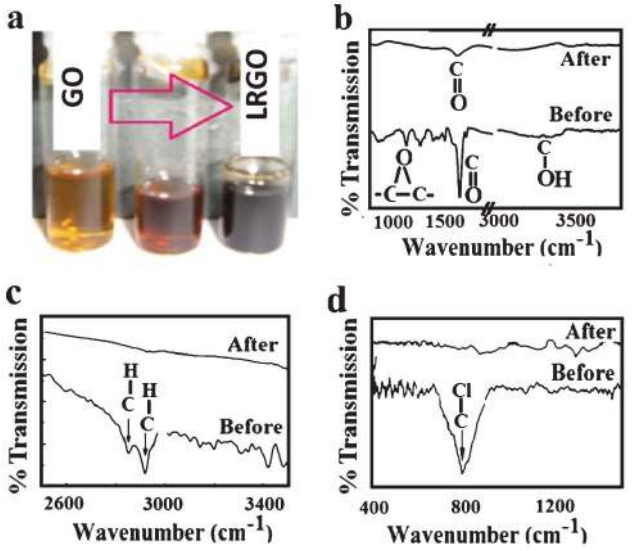

Fig. 14 Laser induced photochemical transformations; (a) photographs of a graphene oxide dispersion before and after two doses of laser irradiation, FTIR spectra for the photochemical transformations before and after laser treatment for (b) graphene oxide, (c) hydrogenated graphene and (d) halogenated graphene. Reprinted with permission from ref. 92. Copyright 2010, Elsevier and ref. 103. Copyright 2011, Royal Society of Chemistry.

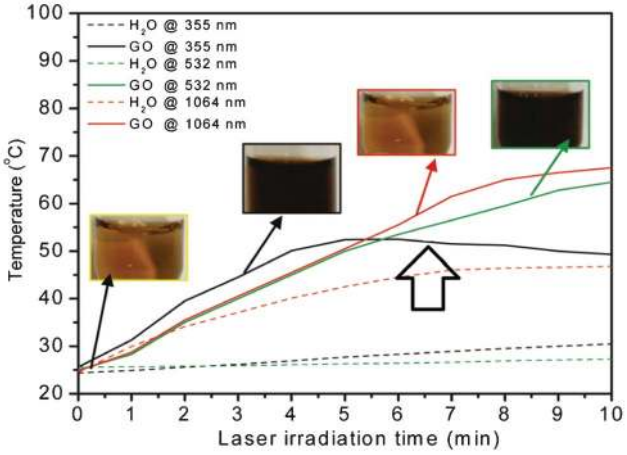

Fig. 15 Temperature changes during laser irradiation of graphite oxide solutions with fundamental (1064 nm) and various harmonics (532 and 355 nm) of the Nd–YAG laser (5 W, 30 Hz). Photographs show the change in the colors of the solutions with laser irradiation. The arrow pointing at the black curve denotes bleaching of the solution after 6 min with 355 nm irradiation (5 W, 30 Hz). The dotted curves show the temperature changes which occur when irradiating the same volume of pure water with the corresponding laser frequency (5 W, 30 Hz). Reprinted with permission from ref. 95. Copyright 2010, American Chemical Society.

would be avoided and also one can achieve graphene devices free from traces of metal. Thus, such catalyst-free laser synthesis of graphene has opened up new dimensions to understanding and it is also expected to impact potential applications.

8. Reduction of graphene oxide

Large scale synthesis of graphene has received much attention due to graphene's potential for applications in catalysis, in nanocomposites as fillers and in various other applications where a large amount of free-standing graphene is required. To this end, the graphene oxide reduction approach is one of the solutions.[59] Most of the reports on chemical approaches rely on hydrazine vapour as a reducing agent. There are of course other reducing agents too. Photocatalytic reduction is also one of the approaches for this goal, where a metal oxide is used as a catalyst for photoreduction.[91] Use of a laser for graphene oxide reduction was first reported by us[92] in 2010, and since then several such reports by other groups have followed.[93–96] Fig. 14(a) shows how a laser changes a yellow coloured aqueous graphene oxide (GO) dispersion first to red and then to a black laser reduced graphene oxide (LRGO) solution. The FTIR spectra in Fig. 14(b) show that due to laser irradiation, oxygen related functionalities disappear. Essentially, high energy photons are capable of cleaving oxygen related functionalities. Thus the use of lasers for graphene oxide reduction eliminates the need for a reducing agent, which was previously used[59] for the purpose of reduction. The laser thus makes the aim of achieving a scalable process for graphene synthesis feasible. Also, the extent of reduction is quite high compared to other contemporary approaches for graphene oxide reduction.

Lasers can be employed for dehydrogenation[5,39] and dehalogenation[5,103] of graphene surfaces. Fig. 14(b), (c) and (d) show the FTIR spectra for pristine graphene oxide and those for the dehydrogenated and dehalogenated samples respectively. Raman spectroscopy has been carried out to show that the defect peaks are considerably reduced after dehydrogenation or dehalogenation. Electrical conductivity measurements also proved that the electrical conductivity of graphene can be restored. Thus it has been successfully demonstrated that lasers exhibit the capability to induce photochemical transformations by effectively cleaving surface bonds. Such photochemical transformations which involve cleaving the bonds from a graphene surface produce heat which can effectively be used to understand the kinetics of photochemical transformations.[5,95] Fig. 15 shows the temperature rise when graphene oxide photochemically transforms to graphene. As can be seen in Fig. 15, in the case of a 355 nm laser, temperature saturation of the dispersion is achieved earlier than in the case where the GO dispersion is treated with a 532 nm laser. Such an observation is actually expected as lasers with higher photon energy (*i.e.* lower wavelength) are capable of cleaving bonds in shorter times, and more effectively. At this point, it should be noted that the bond dissociation energies for bonds such as C–COOH, C–H or C–Cl in open chain aliphatic molecules, and those in 2D graphene sheets, which are a special class of extended aromatic molecules, are drastically different due to the difference in the nature of the bonds between the atoms

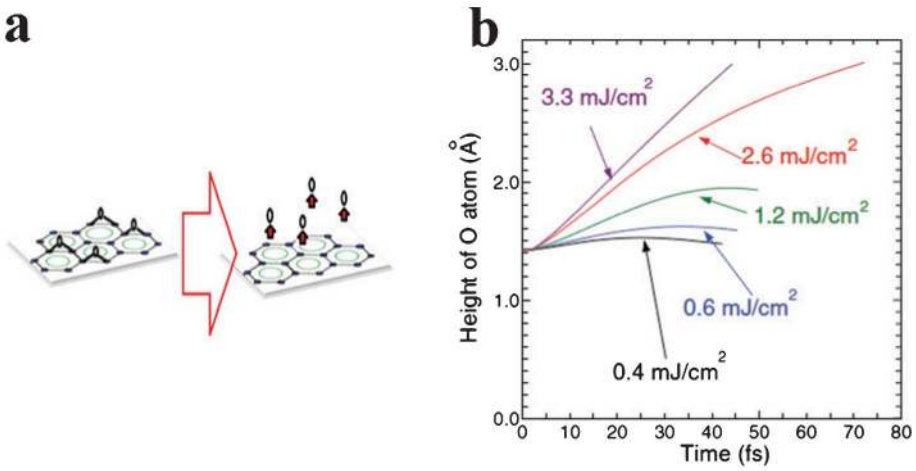

Fig. 16 (a) Schematic of the laser induced deoxygenation of a graphene surface, and (b) DFT calculation of the height of oxygen atoms as a function of time after irradiation with a fs laser pulse. Reprinted with permission from ref. 98. Copyright 2012, American Physical Society.

surrounding that particular bond. Thus by carrying out controlled photothermal effect measurements, one can not only effectively understand the kinetics of such photochemical transformation reactions, but can even evaluate the bond strength for such surface bonds in graphene too.

It should be noted that LRGO has been found to be a good blue emitter,[92] and when combined with yellow emitters such as ZnO nanoparticles, it emits white light. The combination of materials, *i.e.* ZnO + LRGO, is photostable and therefore, the intensity of the white light does not diminish. One can carry out single-step simultaneous reduction of graphene oxide as

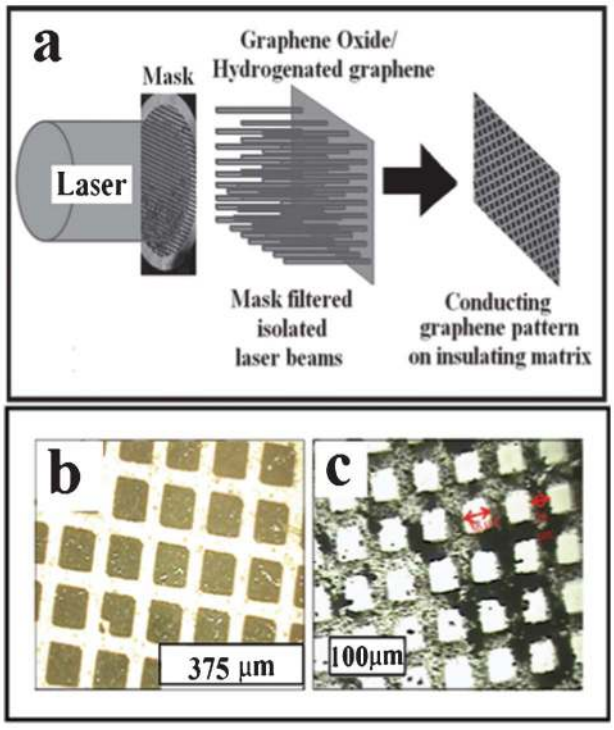

Fig. 17 (a) Schematic diagram showing masked laser patterning (ref. 11), and optical images of laser patterned graphene on a background of (b) insulating GO and (c) hydrogenated graphene. Reprinted with permission from ref. 100. Copyright 2011, American Scientific Publishers.

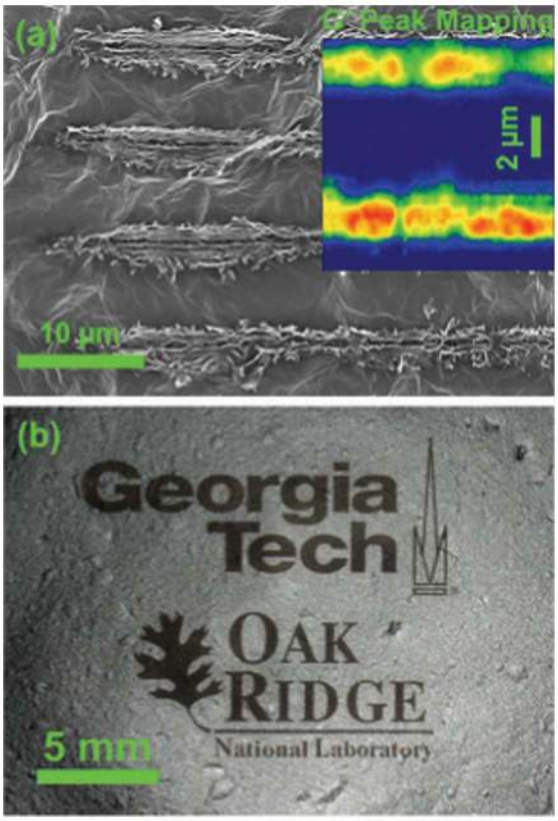

Fig. 18 (a) Graphene lines on a GO background achieved *via* excimer laser based lithography under a high vacuum. The inset is the Raman mapping of the 2D peak along the lithographic lines. (b) Institutional logos printed by excimer laser irradiation of GO under a high vacuum. Reprinted with permission from ref. 101. Copyright 2013, Elsevier.

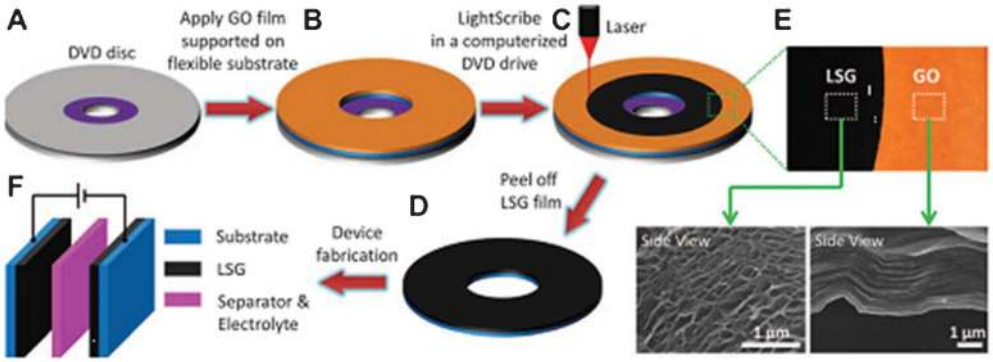

Fig. 19 Schematic diagram for the device fabrication of flexible electrochemical capacitors based on laser scribed graphene on a GO surface. Reprinted with permission from ref. 104. Copyright 2012, The American Association for the Advancement of Science.

well as metal salts using laser irradiation to achieve metal nanoparticle-decorated graphene.[91] Previously, a femtosecond laser was also used for the local reduction of graphene oxide.[97] Recently, Zhang *et al.*[98] have solved a time-dependent Kohn–Sham equation[99] using DFT simulations. The height of the oxygen atom in the epoxy bond is elevated from the graphene sheet over time. At a higher laser power though, the oxygen atom attains a similar height in a considerably shorter time, as can be seen in Fig. 16. As lasers are effective instant tools to convert the insulating background of graphene oxide or hydrogenated graphene into graphene, one can conveniently exploit such capabilities for patterning applications.[100,101] Fig. 17(a) shows a schematic diagram of laser induced masked patterning. Optical images for laser patterned GO and hydrogenated graphene are shown in Fig. 17(b) and (c), respectively. Fig. 18 shows the laser based lithography of graphene lines on a GO background. It has been demonstrated that the 2D peak height increases in the graphene lines scribed on the GO background. It is even possible to conveniently design 3D stacks of graphene and GO at desired locations.[102] Laser reduced graphene oxide (LRGO) has several potential applications. El-Kady *et al.*[104] used such a process for

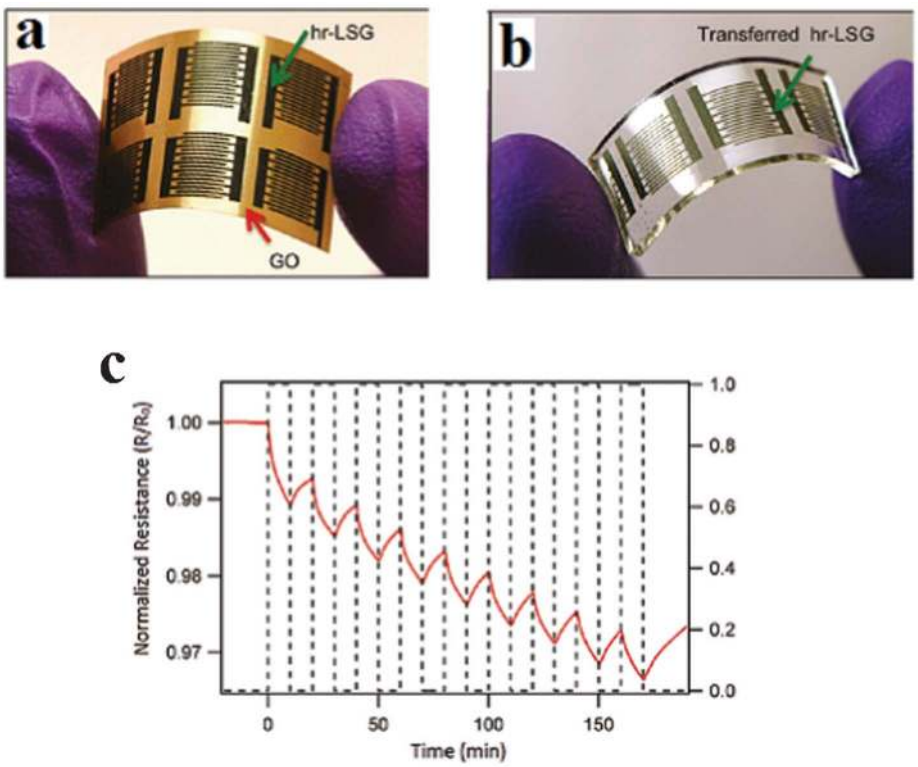

Fig. 20 Laser scribed graphene (LSG) on a graphene oxide film as an all organic flexible electronic device. (a) LSG before transfer, (b) LSG after transfer and (c) resistance *vs.* time plot. Reprinted with permission from ref. 105. Copyright 2012, American Chemical Society.

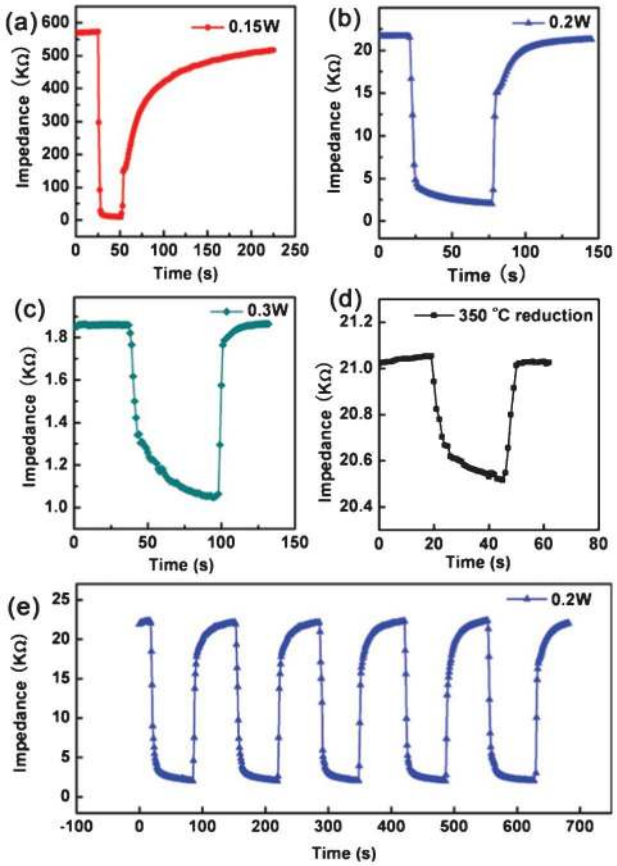

Fig. 21 Humidity sensing by laser reduced graphene oxide reduced at various laser powers. Impedance *vs.* time plot with humidity ''ON'' and ''OFF'' for laser scribed graphene achieved at various power levels (a)–(c), (d) that reduced at 350 °C and (e) consecutive humidity sensing by the LSG sample achieved at a laser power of 0.2 W. Reprinted with permission from ref. 107. Copyright 2012, Elsevier.

the fabrication of high performance capacitors (see Fig. 19). Strong *et al.*[105] and Liu *et al.*[106] have used LRGO as a flexible electronic material (see Fig. 20). Guo *et al.*[107] exploited LRGO for humidity sensing (see Fig. 21). LRGO has also been termed as laser scribed graphene (LSG). Thus, within two years, there has been considerable progress in the laser reduction technique.

9. Graphene nanoribbons from unzipping carbon nanotubes

We have recently reported that lasers can unzip multiwalled carbon nanotubes (MWNTs) into graphene nanoribbons.[108] MWNTs synthesized by CVD, as well as by an arc discharge technique, were successfully unzipped in the solid form under suitable laser conditions. Importantly, doped CNTs such as B- and N-doped CNTs were also unzipped by a laser to achieve doped graphene nanoribbons. Fig. 22 shows TEM images for B-doped MWNT (a) before any treatment and after irradiation at laser energies of (b) 200 mJ and (c) 250 mJ. Achieving doped

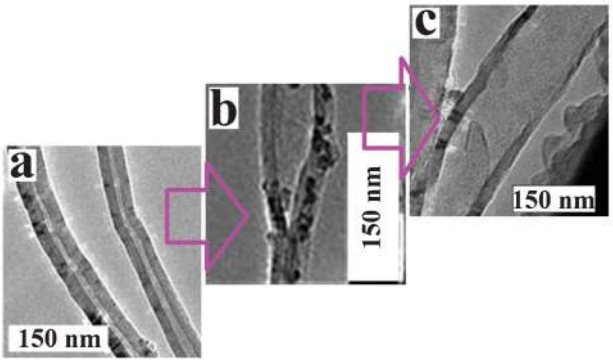

Fig. 22 B-doped graphene nanoribbons achieved *via* laser unzipping of multi-walled carbon nanotubes. (a) Unirradiated MWNTs, and MWNTs laser irradiated at (b) 200 mJ and (c) 250 mJ. Reprinted with permission from ref. 108. Copyright 2011, Royal Society of Chemistry.

graphene nanoribbons by other methods is a really challenging task as already synthesized graphene nanoribbons would buckle or fold when subsequently chemically treated for doping. Also, chemical approaches such as oxidative unzipping[62] of CNTs use $KMnO_4$ along with acids and even after unzipping, the as-formed graphene nanoribbons contain a lot of impurities. In contrast, laser unzipping does not require any reagents as such which makes this technique a clean one. XPS and FTIR characterization revealed that the obtained graphene nanoribbons are chemically pure. Laser irradiation of carbon nanotubes locally heats defect sites which triggers longitudinal unzipping.

10. Inorganic analogues *via* laser exfoliation

Inorganic analogues of graphene, such as insulating BN and semiconducting metal dichalcogenides, can also be exfoliated in a polar medium such as DMF using a laser. We synthesized 2D sheets of BN by a laser exfoliation technique. Fig. 23(a) shows a photograph of a white dispersion of bulk BN in DMF solvent (left) and a transparent supernatant fluid containing laser exfoliated BN sheets (right). Typically exfoliation was achieved by laser irradiation at 1.5 J cm^{-2}, 5 Hz repetition rate for an hour and the top one third of the dispersion was then centrifuged at 3000 rpm for 5 min. Fig. 23(b), (c) and (d) show the FESEM, TEM and AFM images of BN atomic sheets achieved by the laser exfoliation technique. Fig. 23(e) shows the height profile of a BN sheet which shows that it is a single layer BN sheet. Fig. 23(f) shows a characteristic Raman peak for the obtained BN sheet. In a similar fashion, MoS_2, $MoSe_2$, WS_2 and WSe_2 were also exfoliated and have been reported recently.[109] Fig. 24(a) shows a grey coloured dispersion of bulk MoS_2 in DMF (left) and also the transparent supernatant containing laser exfoliated MoS_2 2D sheets (right). Fig. 24(b) shows a TEM image of MoS_2 2D sheets and Fig. 24(c) shows a characteristic Raman spectrum. Fig. 24(d) shows the absorption spectrum of the supernatant containing laser exfoliated

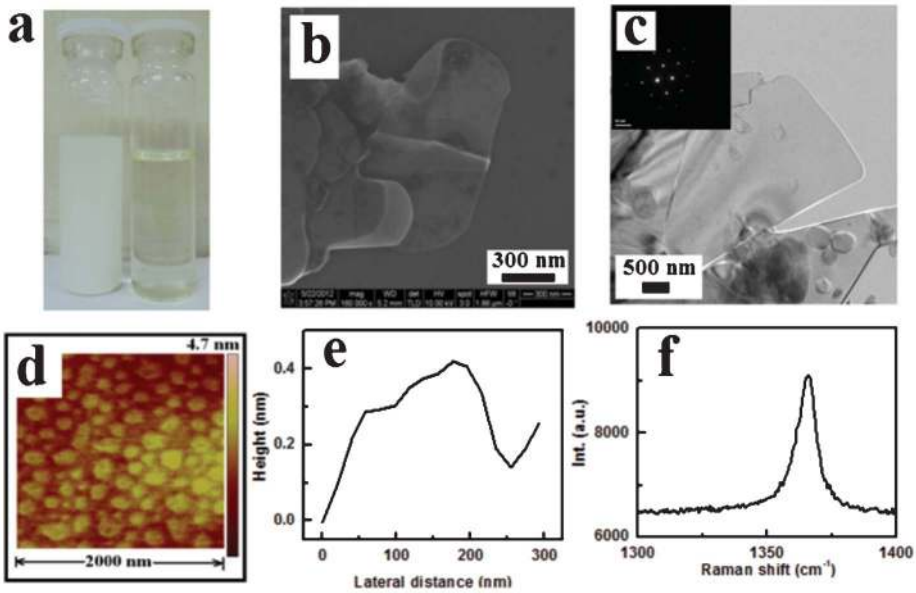

Fig. 23 Laser exfoliation of bulk BN to achieve BN atomic sheets. (a) A photograph of BN bulk powder dispersed in DMF (left) and transparent supernatant fluid achieved after centrifugation of the laser irradiated sample (right). (b) FESEM, (c) TEM, (d) AFM images of the obtained BN atomic sheets. (e) AFM height profile showing a single layer structure and (f) Raman spectrum of the obtained BN sheets. (Author's original research).

2D sheets of MoS_2, which consists of four absorption peaks. Thus, the laser exfoliation technique can be generally applied to several inorganic analogues of graphene. It should be noted that all these inorganic analogues achieved by the laser exfoliation technique are relatively impurity free, and since laser exfoliation is a single step technique the synthesis of such materials has been simplified.

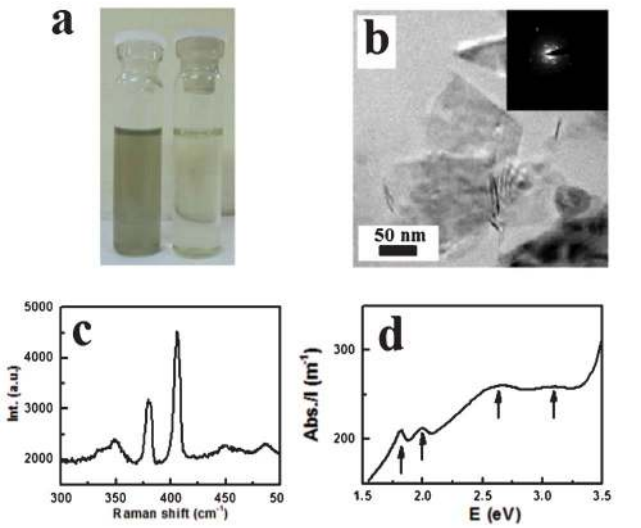

Fig. 24 Laser exfoliation of bulk MoS_2 to achieve MoS_2 atomic sheets. (a) Photograph of MoS_2 bulk powder dispersed in DMF (left) and the transparent supernatant fluid achieved after centrifugation of the laser irradiated sample (right). (b) TEM images and (c) Raman spectrum of the obtained MoS_2 sheets, and (d) the absorption spectrum of the supernatant containing atomic sheets of MoS_2. (a), (c), (d) are the author's original research and Fig. 24(b) is reprinted with permission from ref. 109. Copyright 2012, WILEY-VCH Verlag GmbH & Co. KGaA, Weinheim,

11. Conclusions and outlook

Lasers have been employed to exfoliate 2D atomic sheets. Laser exfoliation provides a scalable instant approach which is universal in nature and can deliver graphene, h-BN, metal dichalcogenides or in general any other 2D materials. Lasers with higher photon energies such as KrF lasers (248 nm) are efficient for cleaving bonds such as C–COOH, C–H, C–Cl, C–C *etc*. Graphene oxide (C–COOH), hydrogenated graphene (C–H) and halogenated graphene (C–Cl) *etc.* have been converted into graphene by exploiting the laser-induced dissociation of these bonds from graphene. Similarly, carbon nanotubes have been unzipped using lasers, which involves breaking the C–C bonds. Such laser-based instant photochemical transformations can be employed for many applications. Lasers have been used for the synthesis of graphene *via* physical vapour deposition from a solid graphite target as well as *via* chemical vapour deposition from gaseous precursors such as methane and hydrogen. Solid carbon sources have also been converted to graphene by lasers. Epitaxial graphene growth on the Si rich surface of SiC has also been achieved by lasers. Fig. 25 gives a glimpse of various laser-based pathways for the synthesis of 2D atomic sheets of graphene and its inorganic analogues. Since laser parameters can be controlled with an amazingly high degree of precision, laser based synthesis of 2D atomic sheets can be exploited for the fabrication of graphene, which could be conveniently integrated into devices. Several device

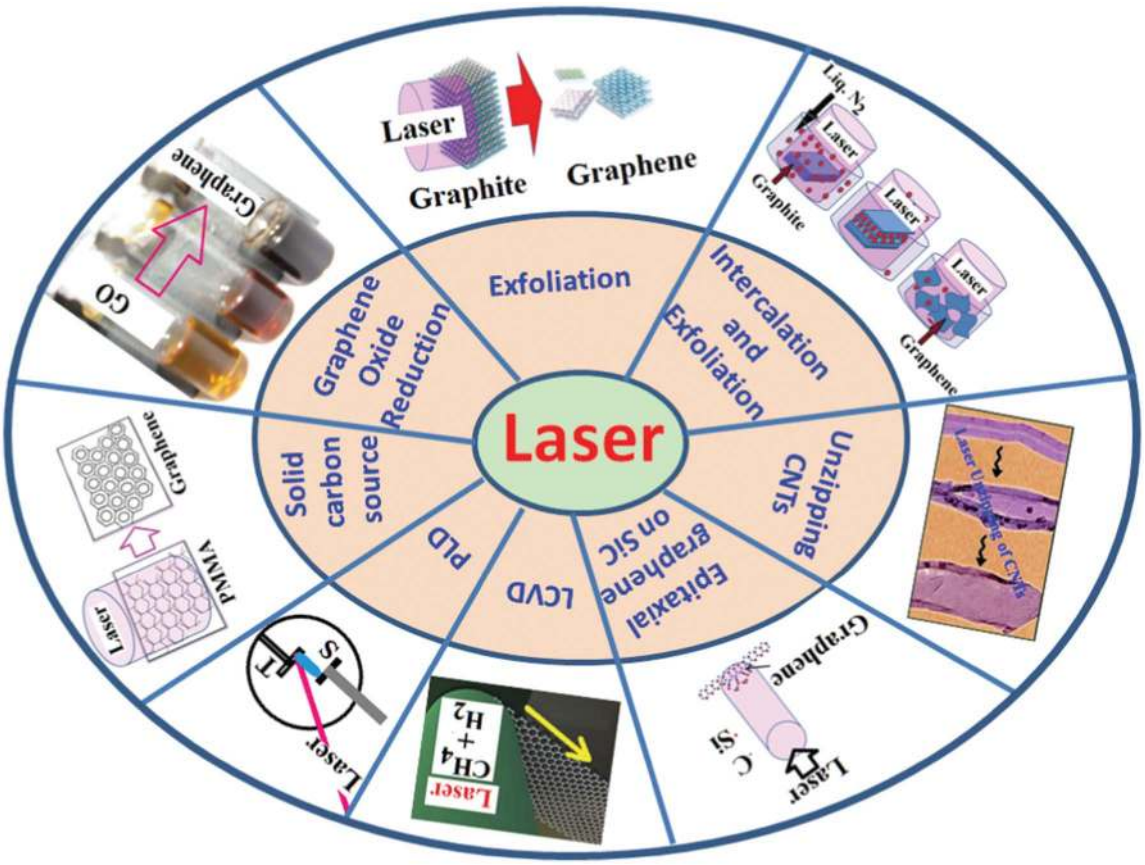

Fig. 25 Overview of various laser-based synthetic approaches for 2D atomic sheets.

applications using laser synthesized graphene have been demonstrated.

Considering the potential applications, it is desirable to obtain graphene with the following properties: (a) minimal number of atomic layers, such as 1–3 layers, (b) homogeneity in the number of layers, (c) minimal defects and (d) catalyst free growth (if possible). Graphene achieved by the LCVD technique, for example, is of high quality and would be the best method for producing graphene for writing circuit elements. For large scale applications in catalysis, the laser reduction of graphene oxide would be capable of supplying large amounts of material. Graphene nanoribbons achieved by laser induced unzipping would be better in quality as unzipping does not involve the use of other chemicals. Laser based graphene growth from a solid precursor on SiO_2 does not actually require any catalyst and therefore, has the potential to achieve metal free graphene which is required to ascertain several of the astonishing properties of graphene in its pure metal-free form. Laser-induced exfoliation of graphite, boron nitride and metal dichalcogenides is yet another approach which can be employed for large scale applications without actually involving any acidic reagents or any catalysts.

Depending on the particular synthetic requirements which are primarily material dependent, a corresponding laser wavelength with a suitable set of laser parameters can conveniently be employed to create the requisite exotic physical or chemical conditions under which a particular photophysical or photochemical transformation can occur. Laser processing for the synthesis of graphene and its inorganic analogues has three remarkable advantages: (a) it is optical in nature and therefore, paves the way for a clean synthetic approach, (b) it is single step and significantly faster processing than other contemporary techniques and (c) the process is scalable. It can be appreciated that the kind of simplicity endowed by laser processing is outstanding, especially in terms of its single-step capability. It is gratifying to note that laser processing technology avoids the use of more chemicals and thus results in the synthesis of 2D atomic sheets with fewer chemical impurities.

Laser irradiation of MgO in the presence of carbon dioxide, the use of lasers for the conversion of various organic solids into graphene, the use of various semiconducting or insulating substrate materials for laser induced growth from solid carbon sources and the use of lasers to achieve graphene from other metal carbide systems are methods where lasers can be employed for graphene synthesis, to name a few. Ultimately, controlled experiments with lasers have to be carried out to explore new pathways for the synthesis of graphene, other 2D materials and their nanocomposites. Laser based novel synthetic approaches do possess exemplary promise for future

material synthesis and thereby create a platform for several emerging applications.

Acknowledgements

I acknowledge Prof. C. N. R. Rao, FRS from International Centre for Materials Science, JNCASR Bangalore, India for scientific discussions. I acknowledge financial support from Raytheon Co., 870 Winter Street, Waltham, MA 02451, USA.

References

1 K. S. Novoselov, A. K. Geim, S. V. Morozov, D. Jiang, Y. Zhang, S. V. Dubonos, I. V. Grigorieva and A. A. Firsov, *Science*, 2004, **306**, 666–669.
2 C. N. R. Rao, K. Biswas, K. S. Subrahmanyam and A. Govindaraj, *J. Mater. Chem.*, 2009, **19**, 2457–2469.
3 C. N. R. Rao, K. S. Subrahmanyam, H. S. S. R. Matte, B. Abdulhakeem, A. Govindaraj, B. Das, P. Kumar, A. Ghosh and D. J. Late, *Sci. Technol. Adv. Mater.*, 2010, **11**, 054502.
4 U. Maitra, H. S. S. R. Matte, P. Kumar and C. N. R. Rao, *Chimia*, 2012, **66**, 941–948.
5 P. Kumar, B. Das, B. Chitara, K. S. Subrahmanyam, K. Gopalakrishnan, S. B. Krupanidhi and C. N. R. Rao, *Macromol. Chem. Phys.*, 2012, **213**, 1146–1163.
6 K. S. Novoselov, V. I. Falko, L. Colombo, P. R. Gellert, M. G. Schwab and K. Kim, *Nature*, 2012, **490**, 192–200.
7 H. C. Neto and K. Novoselov, *Rep. Prog. Phys.*, 2011, **74**, 082501.
8 A. K. Geim, *Science*, 2009, **324**, 1530–1534.
9 C.-C. Lu, Y.-C. Lin, C.-H. Yeh, J.-C. Huang and P.-W. Chiu, *ACS Nano*, 2012, **6**, 4469–4474.
10 C. Lee, X. Wei, J. W. Kysar and J. Hone, *Science*, 2008, **321**, 385–388.
11 S. Bae, H. Kim, Y. Lee, X. Xu, J.-S. Park, Y. Zheng, J. Balakrishnan, T. Lei, H. R. Kim, Y. I. Song, Y.-J. Kim, K. S. Kim, B. Ozyilmaz, J.-H. Ahn, B. H. Hong and S. Iijima, *Nat. Nanotechnol.*, 2010, **5**, 574–578.
12 L. S. Panchakarla, K. S. Subrahmanyam, S. K. Saha, A. Govindaraj, H. R. Krishnamurthy, U. V. Waghmare and C. N. R. Rao, *Adv. Mater.*, 2009, **21**, 4726–4730.
13 A. Das, S. Pisana, B. Chakraborty, S. Piscanec, S. K. Saha, U. V. Waghmare, K. S. Novoselov, H. R. Krishnamurthy, A. K. Geim, A. C. Ferrari and A. K. Sood, *Nat. Nanotechnol.*, 2008, **3**, 210–215.
14 A. H. C. Neto, F. Guinea, N. M. R. Peres, K. S. Novoselov and A. K. Geim, *Rev. Mod. Phys.*, 2009, **81**, 109–162.
15 F. Schwierz, *Nat. Nanotechnol.*, 2010, **5**, 487–496.
16 C. Yan, J. H. Cho and J.-H. Ahn, *Nanoscale*, 2012, **4**, 4870–4882.
17 D. A. Abanin, S. V. Morozov, L. A. Ponomarenko, R. V. Gorbachev, A. S. Mayorov, M. I. Katsnelson, K. Watanabe, T. Taniguchi, K. S. Novoselov, L. S. Levitov and A. K. Geim, *Science*, 2011, **332**, 328–330.
18 D. Pesin and A. H. MacDonald, *Nat. Mater.*, 2012, **11**, 409–416.
19 J. Bai, R. Cheng, F. Xiu, L. Liao, M. Wang, A. Shailos, K. L. Wang, Y. Huang and X. Duan, *Nat. Nanotechnol.*, 2010, **5**, 655–659.
20 J. Yao, J. Lin, Y. Dai, G. Ruan, Z. Yan, L. Li, L. Zhong, D. Natelson and J. M. Tour, *Nat. Commun.*, 2012, **3**, 1101.
21 A. Eichler, J. Moser, J. Chaste, M. Zdrojek, I. W. Rae and A. Bachtold, *Nat. Nanotechnol.*, 2011, **6**, 339–342.
22 C. Chen, S. Rosenblatt, K. I. Bolotin, W. Kalb, P. Kim, I. Kymissis, H. L. Stormer, T. F. Heinz and J. Hone, *Nat. Nanotechnol.*, 2009, **4**, 861–867.
23 A. A. Balandin, *Nat. Mater.*, 2011, **10**, 569–581.
24 Y. M. Zuev, W. Chang and P. Kim, *Phys. Rev. Lett.*, 2009, **102**, 096807.
25 S. Chen, L. Brown, M. Levendorf, W. Cai, S.-Y. Ju, J. Edgeworth, X. Li, C. W. Magnuson, A. Velamakanni, R. D. Piner, J. Kang, J. Park and R. S. Ruoff, *ACS Nano*, 2011, **5**, 1321–1327.
26 M. Liu, X. Yin, E. U. Avila, B. Geng, T. Zentgraf, L. Ju, F. Wang and X. Zhang, *Nature*, 2011, **474**, 64–67.
27 M. Freitag, T. Low, F. Xia and P. Avouris, *Nat. Photonics*, 2013, **7**, 53–59.
28 N. M. Gabor, J. C. W. Song, Q. Ma, N. L. Nair, T. Taychatanapat, K. Watanabe, T. Taniguchi, L. S. Levitov and P. J. Herrero, *Science*, 2011, **334**, 648–652.
29 P. Kumar, L. S. Panchakarla, S. V. Bhat, U. Maitra, K. S. Subrahmanyam and C. N. R. Rao, *Nanotechnology*, 2010, **21**, 385701.
30 F. Bonaccorso, Z. Sun, T. Hasan and A. C. Ferrari, *Nat. Photonics*, 2010, **4**, 611–622.
31 Y.-H. Kim, S.-H. Kwon, J. M. Lee, M.-S. Hwang, J.-H. Kang, W. I. Park and H.-G. Park, *Nat. Commun.*, 2012, **3**, 1123.
32 T.-H. Han, Y. Lee, M.-R. Choi, S.-H. Woo, S.-H. Bae, B. H. Hong, J.-H. Ahn and T.-W. Lee, *Nat. Photonics*, 2012, **6**, 105–110.
33 F. Schedin, A. K. Geim, S. V. Morozov, E. W. Hill, P. Blake, M. I. Katsnelson and K. S. Novoselov, *Nat. Mater.*, 2007, **6**, 652–655.
34 M. Pumera, *Mater. Today*, 2011, **14**, 308–315.
35 Z. Wen, X. Wang, S. Mao, Z. Bo, H. Kim, S. Cui, G. Lu, X. Feng and J. Chen, *Adv. Mater.*, 2012, **24**, 5610–5616.
36 J. J. Yoo, K. Balakrishnan, J. Huang, V. Meunier, B. G. Sumpter, A. Srivastava, M. Conway, A. L. M. Reddy, J. Yu, R. Vajtai and P. M. Ajayan, *Nano Lett.*, 2011, **11**, 1423–1427.
37 H. Wang, Y. Liang, M. Gong, Y. Li, W. Chang, T. Mefford, J. Zhou, J. Wang, T. Regier, F. Wei and H. Dai, *Nat. Commun.*, 2012, **3**, 917.
38 Y. Sun, Q. Wu and G. Shi, *Energy Environ. Sci.*, 2011, **4**, 1113–1132.
39 K. S. Subrahmanyam, P. Kumar, U. Maitra, A. Govindaraj, K. P. S. S. Hembram, U. V. Waghmare and C. N. R. Rao, *Proc. Natl. Acad. Sci. U. S. A.*, 2011, **108**, 2674–2677.
40 S. Patchkovskii, J. S. Tse, S. N. Yurchenko, L. Zhechkov, T. Heine and G. Seifert, *Proc. Natl. Acad. Sci. U. S. A.*, 2005, **102**, 10439–10444.
41 K. Yang, L. Feng, X. Shi and Z. Liu, *Chem. Soc. Rev.*, 2013, **42**, 530–547.
42 Y. Hernandez, V. Nicolosi, M. Lotya, F. M. Blighe, Z. Sun, S. De, I. T. McGovern, B. Holland, M. Byrne, Y. K. Gunko, J. J. Boland, P. Niraj, G. Duesberg, S. Krishnamurthy,

R. Goodhue, J. Hutchison, V. Scardaci, A. C. Ferrari and J. N. Coleman, *Nat. Nanotechnol.*, 2008, **3**, 563–568.
43 J. Chen, M. Duan and G. Chen, *J. Mater. Chem.*, 2012, **22**, 19625–19628.
44 Z. Tang, J. Zhuang and X. Wang, *Langmuir*, 2010, **26**, 9045–9049.
45 E.-Y. Choi, W. S. Choi, Y. B. Lee and Y.-Y. Noh, *Nanotechnology*, 2011, **22**, 365601.
46 N. G. Shang, P. Papakonstantinou, S. Sharma, G. Lubarsky, M. Li, D. W. McNeill, A. J. Quinn, W. Zhou and R. Blackley, *Chem. Commun.*, 2012, **48**, 1877–1879.
47 L. M. Viculis, J. J. Mack, O. M. Mayer, H. T. Hahn and R. B. Kaner, *J. Mater. Chem.*, 2005, **15**, 974–978.
48 K. H. Park, B. H. Kim, S. H. Song, J. Kwon, B. S. Kong, K. Kang and S. Jeon, *Nano Lett.*, 2012, **12**, 2871–2876.
49 K. S. Subrahmanyam, L. S. Panchakarla, A. Govindaraj and C. N. R. Rao, *J. Phys. Chem. C*, 2009, **113**, 4257–4259.
50 K. S. Kim, Y. Zhao, H. Jang, S. Y. Lee, J. M. Kim, K. S. Kim, J. H. Ahn, P. Kim, J. Y. Choi and B. H. Hong, *Nature*, 2009, **457**, 706–710.
51 C. Mattevi, H. Kim and M. Chhowalla, *J. Mater. Chem.*, 2011, **21**, 3324–3334.
52 A. Ismach, C. Druzgalski, S. Penwell, A. Schwartzberg, M. Zheng, A. Javey, J. Bokor and Y. Zhang, *Nano Lett.*, 2010, **10**, 1542–1548.
53 I. Forbeaux, J.-M. Themlin, A. Charrier, F. Thibaudau and J.-M. Debever, *Appl. Surf. Sci.*, 2000, **162**, 406–412.
54 P. N. First, W. A. de Heer, T. Seyller, C. Berger, J. A. Stroscio and J.-S. Moon, *MRS Bull.*, 2010, **35**, 296–305.
55 W. A. de Heer, C. Berger, M. Ruan, M. Sprinkle, X. Li, Y. Hu, B. Zhang, J. Hankinson and E. Conrad, *Proc. Natl. Acad. Sci. U. S. A.*, 2011, **108**, 16900–16905.
56 Z. Sun, Z. Yan, J. Yao, E. Beitler, Y. Zhu and J. M. Tour, *Nature*, 2010, **468**, 549–552.
57 Z. Yan, Z. Peng, Z. Sun, J. Yao, Y. Zhu, Z. Liu, P. M. Ajayan and J. M. Tour, *ACS Nano*, 2011, **5**, 8187–8192.
58 T. Lin, Y. Wang, H. Bi, D. Wan, F. Huang, X. Xie and M. Jiang, *J. Mater. Chem.*, 2012, **22**, 2859–2862.
59 S. Stankovich, D. A. Dikin, R. D. Piner, K. A. Kohlhaas, A. Kleinhammes, Y. Jia, Y. Wu, S. B. T. Nguyen and R. S. Ruoff, *Carbon*, 2007, **45**, 1558–1565.
60 I. Jung, M. Vaupel, M. Pelton, R. Piner, D. A. Dikin, S. Stankovich, J. An and R. S. Ruoff, *J. Phys. Chem. C*, 2008, **112**, 8499–8506.
61 D. R. Dreyer, S. Park, C. W. Bielawski and R. S. Ruoff, *Chem. Soc. Rev.*, 2010, **39**, 228–240.
62 D. V. Kosynkin, A. L. Higginbotham, A. Sinitskii, J. R. Lomeda, A. Dimiev, B. K. Price and J. M. Tour, *Nature*, 2009, **458**, 872–876.
63 D. K. James and J. M. Tour, *Macromol. Chem. Phys.*, 2012, **213**, 1033–1050.
64 A. V. Talyzin, S. Luzan, I. V. Anoshkin, A. G. Nasibulin, H. Jiang, E. I. Kauppinen, V. M. Mikoushkin, V. V. Shnitov, D. E. Marchenko and D. Noreus, *ACS Nano*, 2011, **5**, 5132–5140.
65 H. Terrones, R. Lv, M. Terrones and M. S. Dresselhaus, *Rep. Prog. Phys.*, 2012, **75**, 062501.
66 X. Jia, J. C. Delgado, M. Terrones, V. Meunier and M. S. Dresselhaus, *Nanoscale*, 2011, **3**, 86–95.
67 A. Nag, K. Raidongia, K. P. S. S. Hembram, R. Datta, U. V. Waghmare and C. N. R. Rao, *ACS Nano*, 2010, **4**, 1539–1544.
68 H. S. S. R. Matte, A. Gomathi, A. K. Manna, D. J. Late, R. Datta, S. K. Pati and C. N. R. Rao, *Angew. Chem., Int. Ed.*, 2010, **49**, 4059–4062.
69 J. N. Coleman, M. Lotya, A. O'Neill, S. D. Bergin, P. J. King, U. Khan, K. Young, A. Gaucher, S. De, R. J. Smith, I. V. Shvets, S. K. Arora, G. Stanton, H.-Y. Kim, K. Lee, G. T. Kim, G. S. Duesberg, T. Hallam, J. J. Boland, J. J. Wang, J. F. Donegan, J. C. Grunlan, G. Moriarty, A. Shmeliov, R. J. Nicholls, J. M. Perkins, E. M. Grieveson, K. Theuwissen, D. W. McComb, P. D. Nellist and V. Nicolosi, *Science*, 2011, **331**, 568–571.
70 S. J. Henley, M. J. Beliatis, V. Stolojan and S. R. P. Silva, *Nanoscale*, 2013, **5**, 1054–1059.
71 M. J. Beliatis, S. J. Henley and S. R. P. Silva, *Opt. Lett.*, 2011, **36**, 1362–1364.
72 M. G. Krishna and P. Kumar, Non-lithographic techniques for nanostructuring thin films and surfaces, in *Emerging nanotechnologies for manufacturing*, ed. W. Ahmed and M. J. Jackson, William Andrews Inc. Academic Press, New York, edn. 12009, 1, p. 15838. ISBN 97808155.
73 P. Kumar and M. G. Krishna, *Phys. Status Solidi A*, 2010, **207**, 947–954.
74 P. Kumar, M. G. Krishna and A. Bhattacharya, *J. Nanosci. Nanotechnol.*, 2009, **9**, 3224–3232.
75 P. Kumar, *Nanoscale Res. Lett.*, 2010, **5**, 1367–1376.
76 Y. S. Zhou, W. Xiong, J. Park, M. Qian, M. M. Samani, Y. Gao, L. Jiang and Y. Lu, *J. Laser Appl.*, 2012, **24**, 042007.
77 M. Lenner, A. Kaplan, Ch. Huchon and R. E. Palmer, *Phys. Rev. B: Condens. Matter Mater. Phys.*, 2009, **79**, 184105.
78 Y. Miyamoto, H. Zhang and D. Tomanek, *Phys. Rev. Lett.*, 2010, **104**, 208302.
79 G. H. Han, S. J. Chae, E. S. Kim, F. Guneș, I. H. Lee, S. W. Lee, S. Y. Lee, S. C. Lim, H. K. Jeong, M. S. Jeong and Y. H. Lee, *ACS Nano*, 2011, **5**, 263–268.
80 M. Qian, Y. S. Zhou, Y. Gao, J. B. Park, T. Feng, S. M. Huang, Z. Sun, L. Jiang and Y. F. Lu, *Appl. Phys. Lett.*, 2011, **98**, 173108.
81 G. Compagnini, P. Russo, F. Tomarchio, O. Puglisi, L. D'Urso and S. Scalese, *Nanotechnology*, 2012, **23**, 505601.
82 S. Z. Mortazavi, P. Parvin and A. Reyhani, *Laser Phys. Lett.*, 2012, **9**, 547–552.
83 S. Lee, M. F. Toney, W. Ko, J. C. Randel, H. J. Jung, K. Munakata, J. Lu, T. H. Geballe, M. R. Beasley, R. Sinclair, H. C. Manoharan and A. Salleo, *ACS Nano*, 2010, **4**, 7524–7530.
84 H. Zhang and P. X. Feng, *Carbon*, 2010, **48**, 359–364.
85 K. Wang, G. Tai, K. H. Wong, S. P. Lau and W. Guo, *AIP Adv.*, 2011, **1**, 022141.
86 A. T. T. Koh, Y. M. Foong and H. C. Chua Daniel, *Appl. Phys. Lett.*, 2010, **97**, 114102.
87 J. B. Park, W. Xiong, Y. Gao, M. Qian, Z. Q. Xie, M. Mitchell, Y. S. Zhou, G. H. Han, L. Jiang and Y. F. Lu, *Appl. Phys. Lett.*, 2011, **98**, 123109.
88 J. B. Park, W. Xiong, Z. Q. Xie, Y. Gao, M. Qian, M. Mitchell, M. M. Samani, Y. S. Zhou, L. Jiang and Y. F. Lu, *Appl. Phys. Lett.*, 2011, **99**, 053103.
89 D. Wei and X. Xu, *Appl. Phys. Lett.*, 2012, **100**, 023110.

90 D. Wei, J. I. Mitchell, C. Tansarawiput, W. Nam, M. Qi, P. D. Ye and X. Xu, *Carbon*, 2013, **53**, 374–479.
91 G. Williams, B. Seger and P. V. Kamat, *ACS Nano*, 2008, **2**, 1487–1491.
92 K. S. Subrahmanyam, P. Kumar, A. Nag and C. N. R. Rao, *Solid State Commun.*, 2010, **150**, 1774–1777.
93 P. Kumar, K. S. Subrahmanyam and C. N. R. Rao, *Int. J. Nanosci.*, 2011, **10**, 559–566.
94 D. A. Sokolov, K. R. Shepperd and T. M. Orlando, *J. Phys. Chem. Lett.*, 2010, **1**, 2633–2636.
95 V. Abdelsayed, S. Moussa, H. M. Hassan, H. S. Aluri, M. M. Collinson and M. S. El-Shall, *J. Phys. Chem. Lett.*, 2010, **1**, 2804–2809.
96 L. Huang, Y. Liu, L.-C. Ji, Y.-Q. Xie, T. Wang and W.-Z. Shi, *Carbon*, 2011, **49**, 2431–2436.
97 Y. Zhang, L. Guo, S. Wei, Y. He, H. Xia, Q. Chen, H.-B. Sun and F.-S. Xiao, *Nano Today*, 2010, **5**, 15–20.
98 H. Zhang and Y. Miyamoto, *Phys. Rev. B: Condens. Matter Mater. Phys.*, 2012, **85**, 033402.
99 A. Castro, M. A. L. Marques, J. A. Alonso, G. F. Bertsch and A. Rubio, *Eur. Phys. J. D*, 2004, **28**, 211.
100 P. Kumar, K. S. Subrahmanyam and C. N. R. Rao, *Mater. Express*, 2011, **1**, 252–256.
101 D. A. Sokolov, C. M. Rouleau, D. B. Geohegan and T. M. Orlando, *Carbon*, 2013, **53**, 81–89.
102 H. F. Teoh, Y. Tao, E. S. Tok, G. W. Ho and C. H. Sow, *J. Appl. Phys.*, 2012, **112**, 064309.
103 K. Gopalakrishnan, K. S. Subrahmanyam, P. Kumar, A. Govindaraj and C. N. R. Rao, *RSC Adv.*, 2012, **2**, 1605–1608.
104 M. F. El-Kady, V. Strong, S. Dubin and R. B. Kaner, *Science*, 2012, **335**, 1326–1331.
105 V. Strong, S. Dubin, M. F. El-Kady, A. Lech, Y. Wang, B. H. Weiller and R. B. Kaner, *ACS Nano*, 2012, **6**, 1395–1403.
106 Y. Liu, L. Huang, G. L. Guo, L. C. Ji, T. Wang, Y. Q. Xie, F. Liu and A. Y. Liu, *J. Nanosci. Nanotechnol.*, 2012, **12**, 6480–6483.
107 L. Guo, H.-B. Jiang, R.-Q. Shao, Y.-L. Zhang, S.-Y. Xie, J.-N. Wang, X.-B. Li, F. Jiang, Q.-D. Chen, T. Zhang and H.-B. Sun, *Carbon*, 2012, **50**, 1667–1673.
108 P. Kumar, L. S. Panchakarla and C. N. R. Rao, *Nanoscale*, 2011, **3**, 2127–2129.
109 H. S. S. R. Matte, U. Maitra, P. Kumar, B. G. Rao, K. Pramoda and C. N. R. Rao, *Z. Anorg. Allg. Chem.*, 2012, **638**, 2617–2624.

